

## Electron Spin Density Distribution in the Polymer Phase of CsC<sub>60</sub>: Assignment of the NMR Spectrum

T.M. de Swiet,<sup>1,4,\*</sup> J.L. Yarger,<sup>2,4</sup> T. Wagberg,<sup>3</sup> J. Hone,<sup>3</sup> B.J. Gross,<sup>4</sup> M. Tomaselli,<sup>4</sup>  
J.J. Titman,<sup>1</sup> A. Zettl,<sup>3</sup> and M. Mehring<sup>5</sup>

<sup>1</sup>School of Chemistry, University of Nottingham, Nottingham NG7 2RD, United Kingdom

<sup>2</sup>Department of Chemistry, University of Wyoming, Laramie, Wyoming 82071

<sup>3</sup>Department of Physics, University of California, Berkeley, California 94720

<sup>4</sup>Materials Science Division, E. O. Lawrence Berkeley National Laboratory, Berkeley, California 94720  
and Department of Chemistry, University of California, Berkeley, California 94720

<sup>5</sup>2. Physikalisches Institut, Universität Stuttgart, Pfaffenwaldring 57, D-70550 Stuttgart, Germany  
(Received 19 July 1999)

We present high resolution <sup>133</sup>Cs-<sup>13</sup>C double resonance NMR data and <sup>13</sup>C-<sup>13</sup>C NMR correlation spectra of <sup>13</sup>C enriched samples of the polymeric phase of CsC<sub>60</sub>. These data lead to a partial assignment of the lines in the <sup>13</sup>C NMR spectrum of CsC<sub>60</sub> to the carbon positions on the C<sub>60</sub> molecule. A plausible completion of the assignment can be made on the basis of an *ab initio* calculation. The data support the view that the conduction electron density is concentrated at the C<sub>60</sub> "equator," away from the interfullerene bonds.

PACS numbers: 71.20.Tx, 76.70.Fz

The electronic and magnetic properties of the alkali intercalated fullerides, A<sub>n</sub>C<sub>60</sub>, are still only partly understood. The case A = Rb, Cs, n = 1 has attracted particular interest [1,2]. Above ~350 K, AC<sub>60</sub> adopts an fcc phase with the C<sub>60</sub> molecules rapidly rotating. Annealing below this temperature yields an orthorhombic phase where the molecules polymerize along one direction [3–5]. Quenching through the transition point yields a phase with C<sub>60</sub> dimers [6,7]. Below ~50 K there is a further transition to a magnetically ordered state, which has provoked considerable debate [4,5,8–14].

The basic structural features of the polymer phase, such as the dimensions of the unit cell, C<sub>60</sub> center positions, and the 2 + 2 cycloaddition polymerization along the crystallographic *a* axis are widely supported through x-ray diffraction [3,4], neutron diffraction [15], Raman studies [16–18], inelastic neutron scattering [19], NMR measurements [20–23], and theoretical work [11,24].

However the degree of deformation of the C<sub>60</sub> balls [25] and the rotational orientation of the polymer chains are less well characterized. Neutron diffraction [15] indicated that the polymer chains are randomly oriented although x-ray studies, especially recent single crystal work [26], implied that the polymer chains are uniformly oriented with the cycloaddition planes at 45° to the crystal *b* and *c* axes. With possible strong electron transfer transverse to the chains [11], this type of structural detail is vital to constructing a good model of the electronic properties [27].

NMR has proven a useful probe of structure and electronic properties both for the broader class of alkali intercalated fulleride materials [28] and for AC<sub>60</sub> in particular. The first NMR evidence for *sp*<sup>3</sup> carbons and a broad spin density distribution in AC<sub>60</sub> came from <sup>13</sup>C magic angle spinning (MAS) NMR [20] which was followed by a number of detailed investigations [10,21–23,29–32]. In the

orientationally ordered structures of AC<sub>60</sub> which have been proposed, there are 16 inequivalent <sup>13</sup>C nuclei, as shown in Fig. 1. A central task is to assign the peaks in the <sup>13</sup>C NMR spectrum to the different <sup>13</sup>C positions. This step is significant since it yields a map of the hyperfine coupling constant around the fullerene, against which models of the band structure can be tested. Furthermore, such an assignment is a prerequisite to any more detailed NMR study of internuclear distances which might resolve the structural questions. In this paper we report an attempt to make this assignment.

In order to obtain sufficient sensitivity, samples of CsC<sub>60</sub> were synthesized using <sup>13</sup>C enriched fullerenes. These were prepared by packing and sintering <sup>13</sup>C enriched amorphous carbon into graphite tubes to create <sup>13</sup>C enriched carbon rods. The fullerenes were subsequently produced by arcing a 60 A, 25 V dc current between an ordinary

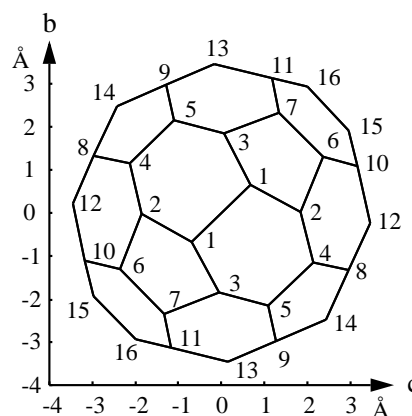


FIG. 1. Inequivalent carbon positions projected into the crystallographic *bc* plane. The polymer chain runs along the orthogonal *a* axis [3]. Sites 1–14 contain four <sup>13</sup>C atoms per C<sub>60</sub> ball, and sites 15–16 contain two <sup>13</sup>C atoms per C<sub>60</sub> ball.

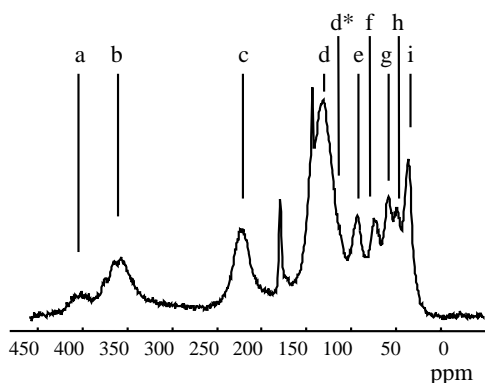


FIG. 2.  $^{13}\text{C}$  spectrum of sample 1 taken with a Varian/Chemagnetics 3.2 mm MAS probe and CMX spectrometer at a field of 7.05 T, 24 kHz MAS, and 2 s pulse delay.

graphite electrode and a  $^{13}\text{C}$  enriched rod under a  $\sim 3$  psi He atmosphere. Percent enrichment was verified by mass spectroscopy. The  $\text{C}_{60}$  was isolated from the soot via filtration and flash chromatography. Stoichiometric amounts of the enriched fullerenes and cesium were mixed, heated for one week at 350  $^{\circ}\text{C}$ , and then cooled to room temperature over 2 days. Both 50%  $^{13}\text{C}$  enriched  $\text{CsC}_{60}$  (sample 1) and 8%  $^{13}\text{C}$  enriched  $\text{CsC}_{60}$  (sample 2) were prepared.

Figure 2 shows the one-dimensional (1D)  $^{13}\text{C}$  magic angle spinning spectrum of sample 1. The spectrum can be fitted well to 11 Lorentzian peaks. Nine of these peaks are characteristic of the polymer phase of  $\text{CsC}_{60}$  (see Table I) while the peaks at 179 and 143 ppm are remnants of the cubic phase of  $\text{CsC}_{60}$  and  $\alpha\text{-C}_{60}$ , respectively [22,23,30]. Previous researchers [30] have been able to identify the shoulder, marked  $d^*$ , on the side of peak  $d$  with a separate Lorentzian. Our data do not permit a meaningful fit of this shoulder. Nevertheless, in 2D spectra, resolved cross peaks are visible between peak  $g$  and region  $d^*$ , centered on 118 ppm, which is in close agreement to the value of 117 ppm given in Ref. [30]. We have observed that peaks  $f-i$  move, and can obscure each other, as the spinning

speed is varied. This effect probably results from spinning speed affecting sample temperature, and thus Knight shifts, and may explain why peak  $h$  was seen in Fig. 1b of Ref. [23] but not in Ref. [30]. Since there are fewer resolved NMR peaks than  $^{13}\text{C}$  positions, some peaks must correspond to more than one position. The poor resolution must be derived from sample disorder, such as incomplete polymerization, and leads to systematic errors in the peak intensities in Table I, because the individual line shapes are not known *a priori*. This is a particular problem with peaks  $a$  and  $b$ , and for much of what follows we will combine them as one peak.

In order to identify pairs of bonded  $^{13}\text{C}$  sites, we performed  $^{13}\text{C}$  MAS dipolar correlation spectroscopy [33]. Here, the  $^{13}\text{C}$  spins were allowed to precess freely for a time  $t_1$ . Next, the  $^{13}\text{C}$ - $^{13}\text{C}$  dipole-dipole interaction, normally removed by MAS, was recoupled using the POST-C7 [34] pulse sequence, for a mixing time equal to four MAS periods. This allows spin polarization to be transferred between  $^{13}\text{C}$  nuclei which are sufficiently close in space. An analysis of the structure in Fig. 1 shows that there is only a measurable transfer between directly bonded  $^{13}\text{C}$  spins. After the mixing time, the signal is recorded as a function of  $t_2$ . Double Fourier transformation of the data reveals a plot with peaks along the diagonal,  $\omega_1 = \omega_2$ , resulting from polarization which is not transferred during the mixing period, and cross peaks resulting from polarization transfer between directly bonded carbon sites. The spectra were “double quantum filtered,” which partly suppresses the intensity of the diagonal peaks and removes any contribution from isolated  $^{13}\text{C}$  nuclei.

One such correlation spectrum is shown in Fig. 3. Note that the double quantum filter has completely suppressed the impurity peaks. The fullerenes are rapidly tumbling in these materials, which greatly reduces the effective dipole couplings. Artifacts in the spectrum, such as “ $t_1$  noise,” spinning sidebands, and ridges along  $\omega_1 = 0$  and the antidiagonal, were distinguished from true cross peaks by

TABLE I. Shift ( $\delta$ ) and intensity, normalized to 60 ( $\#/\text{C}_{60}$ ) of the  $^{13}\text{C}$  lines in the MAS spectrum of  $\text{CsC}_{60}$ . 24 kHz MAS and a 2 s pulse delay were used for sample 1 ( $\delta_1$ ). 16.5 kHz and 1 s were used for sample 2 ( $\delta_2$ ). For comparison we show the data of Brouet *et al.* ( $\delta_B$ ) [30], assuming that peak  $d$  is the sum of peaks  $D$  and  $E$  of that work, and the sum of  $g$  and  $h$  is peak  $Y$ .  $R_{\text{CsC}}$  represents the experimental  $^{13}\text{C}$ - $^{13}\text{C}$  REDOR fraction times  $[(10 \text{ ms})/t]^2$ , at short echo times  $t$ . The last line lists the  $^{13}\text{C}$  cross peaks which occur between pairs of lines  $a, \dots, i$  (top row) in  $^{13}\text{C}$ - $^{13}\text{C}$  correlation spectra (Fig. 3) due to spin polarization transfer between nearest neighbor carbons.

	$a$	$b$	$c$	$d$	Line $e$	$f$	$g$	$h$	$i$
$\delta_1$ (ppm)	407	359	222	132	93	74	59	49	36
$\#/\text{C}_{60}$	1.0	9.6	7.9	24.2	2.9	3.4	3.4	2.6	5.0
$\delta_2$ (ppm)	398	359	222	133	97	80	60	46	35
$\#/\text{C}_{60}$	4.8	3.8	11.6	18.8	3.0	2.4	7.4	5.2	2.95
$\delta_B$ (ppm)	397	357	220	126	94	77		55	35
$\#/\text{C}_{60}$	7.1	3.5	8	18.2	2.8	1.5		12.6	4
Expt. $R_{\text{CsC}}$	2.5	0.8	2.0	2.5	0.5	5.8	2.1	0.9	0.7
Cross Peaks	$d g$	$d g$	$e f$	$a/b e$	$c d$	$c d$	$a/b$	$a/b$	$e$
	$h$	$h$	$g h$	$f h$	$i$	$i$	$c d^*$	$c d$	$f$

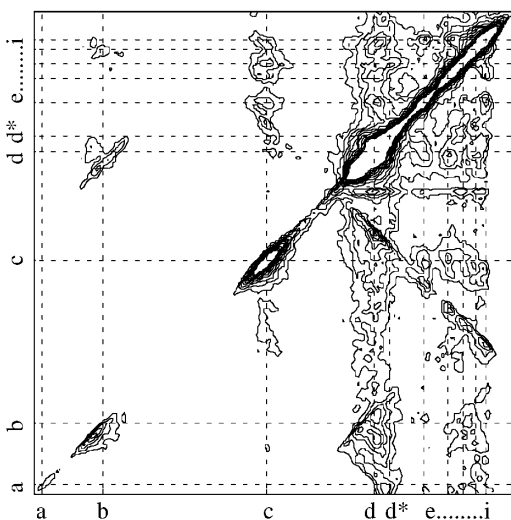


FIG. 3. A 2D  $^{13}\text{C}$ - $^{13}\text{C}$  correlation spectrum of  $\text{CsC}_{60}$ , taken with a Varian/Chemagnetics 3.2 mm MAS probe and CMX spectrometer at 7.05 T, 17 kHz MAS, and 2 s pulse delay. The dotted lines show the positions of ten Lorentzians obtained from a fit to an ordinary 1D spectrum at 17 kHz MAS. The spectrum is 417 ppm wide.

varying the rf carrier position, and spinning speed from 17–19 kHz. This causes the artifacts to move relative to the rest of the spectrum.

The rotational echo double resonance (REDOR) experiment aims to measure distances between the nuclei of different isotopes under MAS conditions by recoupling the heteronuclear dipole-dipole interaction [35]. The signal of a Hahn spin echo on  $^{13}\text{C}$  sites was measured with ( $S_e$ ) and without ( $S_0$ ) a train of rotor synchronized  $\pi$  pulses on the  $^{133}\text{Cs}$  channel. At short echo times  $t$ , the REDOR fraction on the  $i$ th  $^{13}\text{C}$  site is given by

$$R_{\text{CsC}} = \frac{S_0^i - S_e^i}{S_0^i} = \frac{1}{45\pi^4} \mu_0^2 \gamma_C^2 \gamma_{\text{Cs}}^2 \hbar^2 t^2 I(I+1) \sum_j \frac{1}{r_{ij}^6}. \quad (1)$$

Here  $r_{ij}$  is the distance between the  $i$ th  $^{13}\text{C}$  site and the  $j$ th  $^{133}\text{Cs}$  site, the sum running over all of the  $^{133}\text{Cs}$  positions in the lattice, and  $I = 7/2$ , the spin of  $^{133}\text{Cs}$ . Experimental values of  $R_{\text{CsC}}$  for the nine peaks in the  $^{13}\text{C}$  MAS NMR spectrum are given in Table I, and theoretical values based on the 16 sites of the x-ray structure [3] are shown in Table II. The experimental data were taken at

16.5 kHz MAS, with 8.6  $\mu\text{s}$  180° pulses on Cs, and the XY8 phase cycle [36] was used. Unfortunately, quantitative analysis of this data is difficult due to imperfections in the applied  $^{133}\text{Cs}$   $\pi$  pulses due to the  $^{133}\text{Cs}$  quadrupole coupling,  $\nu_Q \sim 12$  kHz [30]. This tends to reduce the measured REDOR fraction. Nevertheless, it is reasonable to assume that the peaks in the carbon spectrum with large REDOR fractions are relatively close to the Cs lattice positions. Thus REDOR may be used as a guide between possible spectral assignments derived from the 2D spectra.

The first step in the NMR assignment is to decide which peaks are coupled to each other in the 2D spectra. The results are given in Table I, where it has been assumed that peaks  $e$ – $i$  contain no more than four carbons per  $\text{C}_{60}$ , and so can have no more than three cross peaks each. Two independent groups [22,23], have already concluded that NMR peak  $i$  corresponds to site 1 of the crystal structure, which is the  $sp^3$  coordinated site in the  $\text{C}_{60}$ - $\text{C}_{60}$  bond. The cross peaks listed in Table I then imply that peaks  $e$  and  $f$  must be responsible for crystal sites 2 and 3. Now site 3 has the strongest REDOR effect of all and site 2 has the weakest. This is consistent with  $f$  having the strongest REDOR effect and peak  $e$  having the weakest. We therefore assign  $e$  to 2 and  $f$  to 3.

From this point the NMR data leads to two groups of possible assignments characterized by whether sites 4 and 5 are assigned to peak  $c$  (choice A) or peak  $d$  (choice B). With choice A, one finds sites 6, 7, 8, 9, 12, 13, 14 are assigned to peaks  $d, d, h, g, d, d^*, a/b$ , respectively, and sites 10, 11, 15, and 16 must be allocated in some way to the remainder of peaks  $a/b$  and  $d$ . In choice B, sites 6, 7, 10, 11 are assigned to peaks  $c, c, h, g$ , and either site 13 or 16 is peak  $d^*$  which leads to several ways of assigning sites 8, 9, 12, 14, 15 to peaks  $a/b$  and  $d$ . We note that in all possible assignments the peaks  $a/b$  must lie in the band of sites 8–16 around the  $\text{C}_{60}$  “equator.”

In order to attempt the choice between A or B, we have performed density functional calculations (DFT) on a  $\text{C}_{60}$  trimer which forms a piece of the polymer chain. The trimer is terminated at each end with cycloaddition to  $\text{CH}_2$ - $\text{CH}_2$  groups. The calculation was performed with GAUSSIAN 98 using the BLYP/STO-3G parameter specification [37].

The measured NMR shift is the sum of the chemical and Knight shifts. The chemical shift is due to the local field at the nucleus of the filled orbital electrons which

TABLE II. Site selective assignment of different parameters.  $R_{\text{CsC}}$  represents the theoretical  $^{133}\text{Cs}$ - $^{13}\text{C}$  REDOR fraction data times  $[(10 \text{ ms})/t]^2$ . The basis for the assignment of the  $^{13}\text{C}$  NMR lines  $a, \dots, i$  to the carbon sites is described in the text. The last two rows correspond to the experimental Knight shift and spin density  $\rho_{\text{spin}}(j) = K(j)/\sum_{j=1}^{60} |K(j)|$  for the carbon sites  $j = 1, \dots, 16$ .

	Site															
	1	2	3	4	5	6	7	8	9	10	11	12	13	14	15	16
Theor. $R_{\text{CsC}}$	5.8	3.4	19.1	4.3	14.3	4.4	13	5.5	9.6	6.8	9.3	14	8.4	4.1	5.1	4.0
$^{13}\text{C}$ lines	$i$	$e$	$f$	$c$	$c$	$d$	$d$	$h$	$g$	$b$	$b$	$d$	$d$	$a$	$d$	$d$
$K_i$ (ppm)	-1.5	-48	-66	79	79	-11	-11	-96	-84	216	216	-11	-11	260	-11	-11
$\rho_{\text{spin}} \times 100$	0.0	-1.0	-1.40	1.7	1.7	-0.2	-0.2	-2.0	-1.7	4.5	4.5	-0.2	-0.2	5.4	-0.2	-0.2

are perturbed by the external magnetic field. For aromatic carbons, such as sites 2–16 in  $AC_{60}$ , this is typically 110–170 ppm [38]. Site 1, which is  $sp^3$  coordinated, is expected to have a chemical shift of 30–45 ppm [38]. The Knight shift is due to the hyperfine coupling of the nucleus to the conduction electrons which are polarized by the magnetic field. From Table I, peaks  $a$ ,  $b$ , and  $c$  have shifts which are clearly outside the ordinary chemical shift range, and so must have substantial positive hyperfine couplings. Indeed, in Ref. [23], peaks  $a/b$  and  $c$  were found to have hyperfine couplings of 7.6 and 2.2 MHz, respectively. In the calculation, five sites have by far the largest positive hyperfine couplings—site 14, with 6.6 MHz, sites 10 and 11 with 6.81 MHz, and sites 4 and 5 with 2.6 MHz. This implies the assignment of sites 10, 11, and 14 with peaks  $a/b$ , and sites 4 and 5 with  $c$ . For convenience we assign site 14 to peak  $a$ , and sites 10 and 11 to peak  $b$ , although, as mentioned earlier, we cannot reliably distinguish these two peaks. Furthermore, this assignment is consistent with the A assignment from the NMR data described above, which then becomes unique. The results are listed in Table II. Note that a more detailed comparison between theory and experiment clearly requires a calculation that includes the effects of conduction between the polymer chains and the effect of the crystal field. This is evident from the NMR data which indicate that crystal sites 2 and 3 correspond to different peaks in the spectrum, and the symmetry between these two sites is only broken by the crystal field.

With the NMR assignment in place, it is now possible to estimate the Knight shift at each  $^{13}C$  site in the crystal structure. The Knight shift is obtained by subtracting the chemical shift from the total NMR shift. The values are shown in Table II, where the chemical shift has been estimated at 37 ppm at site 1 and 143 ppm at the remaining sites, and the measured total shifts are averaged over samples 1 and 2. Since the Knight shift is directly proportional to the carbon  $2s$ -spin density we can extract a normalized spin density at site  $j$  by  $\rho(j) = K(j)/\sum_{j=1}^{60} \times |K(j)|$  as is summarized in the last row of Table II. Here we have assumed for simplicity that  $\sum_{j=1}^{60} |\rho(j)| = 1$ .

The distribution of the spin density  $\rho(j)$  on the  $C_{60}$  molecule represents in a way the local conduction electron wave function. Our NMR data analysis shows clearly that it is concentrated near the equator of the  $C_{60}$  molecule and away from the polymer bond. This is in agreement with previous theoretical work [11,27], where the valence electrons of the site  $C1$  carbons are used in the  $C_{60}$ - $C_{60}$  bond and hardly contribute to the conduction band, and the additional electron from the alkali atom resides mainly in a belt around the equator. This provides strong experimental evidence for substantial transverse coupling between polymer chains, and supports the notion that polymer fullerenes have fully 3D electronic properties, as opposed to the 1D model [4]. Finally, we note that the very different measured REDOR fractions on sites 2 and 3 are strong further evidence that the polymer chains are oriented at  $\theta = 45^\circ$

to the crystal  $b$  and  $c$  axes. A calculation based on Eq. (1) shows that the REDOR fractions of these two sites are the same at  $\theta = 0^\circ$  and  $90^\circ$ , and are most different at  $\theta = 45^\circ$ .

This work was supported, in part, by the Director, Office of Basic Energy Sciences, Material Science Division of the U.S. Department of Energy under Contract No. DE-AC0376SF00098. J.L.Y. thanks the National Science Foundation, Grant No. dge-9818238, for support. M.M. acknowledges support from the Deutsche Forschungsgemeinschaft and the Fonds der Chemischen Industrie.

\*Electronic address: thomas.de.swiet@nottingham.ac.uk

- [1] J. Winter and H. Kuzmany, *Solid State Commun.* **84**, 935 (1992).
- [2] Q. Zhu *et al.*, *Phys. Rev. B* **47**, 13 948 (1993).
- [3] P. W. Stephens *et al.*, *Nature (London)* **370**, 636 (1994).
- [4] O. Chauvet *et al.*, *Phys. Rev. Lett.* **72**, 2721 (1994).
- [5] S. Pekker *et al.*, *Solid State Commun.* **90**, 349 (1994).
- [6] G. Oszlanyi *et al.*, *Phys. Rev. B* **51**, 12 228 (1995).
- [7] Q. Zhu, D. E. Cox, and J. E. Fischer, *Phys. Rev. B* **51**, 3966 (1995).
- [8] V. A. Atsarkin, V. V. Demidov, and G. A. Vasneva, *Phys. Rev. B* **56**, 9448 (1997).
- [9] F. Bommeli *et al.*, *Phys. Rev. B* **51**, 14 794 (1995).
- [10] V. Brouet *et al.*, *Phys. Rev. Lett.* **76**, 3638 (1996).
- [11] S. C. Erwin, G. V. Krishna, and E. J. Mele, *Phys. Rev. B* **51**, 7345 (1995).
- [12] M. Fally and H. Kuzmany, *Phys. Rev. B* **56**, 13 861 (1997).
- [13] A. Janossy *et al.*, *Phys. Rev. Lett.* **79**, 2718 (1997).
- [14] M. Bennati *et al.*, *Phys. Rev. B* **58**, 15 603 (1998).
- [15] J. R. Fox *et al.*, *Chem. Phys. Lett.* **249**, 195 (1996).
- [16] D. Bormann *et al.*, *Phys. Rev. B* **54**, 14 139 (1996).
- [17] J. L. Sauvajol *et al.*, *Phys. Rev. B* **56**, 13 642 (1997).
- [18] M. C. Martin *et al.*, *Phys. Rev. B* **51**, 3210 (1995).
- [19] H. Schober *et al.*, *Phys. Rev. B* **56**, 5937 (1997).
- [20] T. Kälber, G. Zimmer, and M. Mehring, *Z. Phys. B* **27**, 2 (1995).
- [21] T. Kälber, G. Zimmer, and M. Mehring, *Phys. Rev. B* **51**, 16 471 (1995).
- [22] H. Alloul *et al.*, *Phys. Rev. Lett.* **76**, 2922 (1996).
- [23] K.-F. Thier *et al.*, *Phys. Rev. B* **53**, R496 (1996).
- [24] S. Pekker, G. Oszlanyi, and G. Faigel, *Chem. Phys. Lett.* **282**, 435 (1998).
- [25] C. H. Choi and M. Kertesz, *Chem. Phys. Lett.* **282**, 318 (1998).
- [26] P. Launois *et al.*, *Phys. Rev. Lett.* **81**, 4420 (1998).
- [27] K. Tanaka *et al.*, *Chem. Phys. Lett.* **272**, 189 (1997).
- [28] C. H. Pennington and V. A. Stenger, *Rev. Mod. Phys.* **68**, 855 (1996).
- [29] R. Tycko *et al.*, *Phys. Rev. B* **48**, 9097 (1993).
- [30] V. Brouet *et al.*, *Appl. Phys. A* **64**, 289 (1997).
- [31] V. Brouet *et al.*, *Physica (Amsterdam)* **235C**, 2481 (1994).
- [32] P. Auban-Senzier *et al.*, *J. Phys. I (France)* **6**, 2181 (1996).
- [33] See, e.g., H. Geen *et al.*, *J. Magn. Reson.* **125**, 224 (1997).
- [34] M. Hohwy *et al.*, *J. Chem. Phys.* **108**, 2686 (1998).
- [35] T. Gullion and J. Schaefer, *J. Magn. Reson.* **81**, 196 (1989).
- [36] T. Gullion and J. Schaefer, *J. Magn. Reson.* **92**, 439 (1991).
- [37] M. J. Frisch *et al.*, Gaussian Inc., Pittsburgh, PA, 1998.
- [38] G. C. Levy, R. L. Lichter, and G. L. Nelson, *Carbon 13 NMR Spectroscopy* (Wiley, New York, 1980).